

Title Page

New multifunctional hybrids as modulators of apoptosis markers and topoisomerase II in breast cancer therapy: Synthesis, characterization, *in vitro*, and *in-silico* studies

Heba W. Alhamdi¹, Mohammad Y. Alfaifi^{2,3}, Ali A Shati^{2,3}, Serag Eldin I. Elbehairi^{2,3,4}, Mohammed Er-rajy⁵, Reda F. M. Elshaarawy^{6,7,*}, Yasser A. Hassan⁸, Rozan Zakrya⁹

¹ College of Sciences, Biology Department, King Khalid University, Abha 61413, Saudi Arabia.

² King Khalid University, Faculty of Science, Biology Department, Abha 9004, Saudi Arabia.

³ Tissue Culture and Cancer Biology Research Laboratory, King Khalid University, Abha, 9004, Saudi Arabia

⁴ Cell Culture Lab, Egyptian Organization for Biological Products and Vaccines (VACSERA Holding Company), 51 Wezaret El-Zeraa St., Agouza, Giza, Egypt.

⁵ LIMAS Laboratory, Faculty of Sciences Dhar El Mahraz, Sidi Mohamed Ben Abdellah University, Fez, Morocco.

⁶ Department of Chemistry, Faculty of Science, Suez University, 43533 Suez, Egypt.

⁷ Institut für Anorganische Chemie und Strukturchemie, Heinrich-Heine Universität Düsseldorf, Düsseldorf, Germany.

⁸ Department of pharmaceuticals, Faculty of Pharmacy, Delta University for Science and Technology, Gamasa, Egypt.

⁹ Chemistry department, Faculty of Science, Port-Said University, Port-Said, Egypt; rzakrya@yahoo.com

* Correspondence: RFME, reda.elshaarawy@suezuniv.edu.eg

Contents

1. Materials and Instrumentation
2. Preparation of benzenediazonium chloride
3. Preparation of 7-hydroxy-4-methylquinolin-2(1H)-one (HMQ)
4. Figures Captions
5. Tables Captions

1. Materials and Instrumentation

1.1. Materials

Chemicals were obtained from the following suppliers and used without further purification: *o*-vanillin, (Roth), anhydrous zinc chloride (ZnCl_2) (GRÜSSING GmbH), thiosemicarbazide hydrochloride (**3**) (TCI), potassium thiocyanate (KSCN), anhydrous potassium carbonate (K_2CO_3), sodium bicarbonate (NaHCO_3), sodium sulphate anhydrous (Na_2SO_4), sodium hydroxide (NaOH) and 3% hydrogen peroxide (H_2O_2) (ADWIC).

1.2. Instrumentation

Melting points (uncorrected) were determined in open glass capillaries on a Gallenkamp melting point apparatus. Elemental analyses for C, H, N and S were performed with a Perkin–Elmer 263 elemental analyzer. FT-IR spectra were recorded on a BRUKER Tensor-37 FT-IR spectrophotometer in the range 400–4000 cm^{-1} as KBr discs or in the 4000–550 cm^{-1} region with 2 cm^{-1} resolution with an ATR (attenuated total reflection) unit (Platinum ATR-QL, Diamond). For signal intensities the following abbreviations were used: br (broad), sh (sharp), w (weak), m (medium), s (strong), vs (very strong). NMR-spectra were obtained with a Bruker Avance DRX200 (200 MHz for ^1H) or Bruker Avance DRX500 (500 MHz for ^{13}C) spectrometer with calibration to the residual proton solvent signal in DMSO- d_6 (^1H NMR: 2.52 ppm, ^{13}C NMR: 39.5 ppm), CDCl_3 (^1H NMR: 7.26 ppm, ^{13}C NMR: 77.16 ppm) against TMS with $\delta = 0.00$ ppm. Multiplicities of the signals were specified s (singlet), d (doublet), t (triplet), q (quartet) or m (multiplet). The mass spectra of the synthesized salicylaldehyde ionic liquids (Sal-ILs) were acquired in the linear mode for positive ions on a BRUKER Ultraflex MALDI-TOF instrument equipped with a 337 nm nitrogen laser pulsing at a repetition rate of 10 Hz.

2. Preparation of benzenediazonium chloride

An aqueous solution of $\text{PhN}_2^+\text{Cl}^-$ is obtained by adding a stoichiometric amount of NaNO_2 at 0–5 °C to the solution obtained from aniline and excess hydrochloric acid in water. An excess of nitrite ions at the end of the reaction should be avoided, since they reduce the stability of the diazonium salt solution and can interfere with some further transformations.

3. Preparation of 7-hydroxy-4-methylquinolin-2(1H)-one (HMQ)

A mixture of 3-aminophenol (20.0 g, 183.3mmol) and ethyl acetoacetate (23.3mL, 183.3 mmol) was heated at 150 °C for 20 h to give a yellow sticky mass which after cooling solidified upon treatment with methanol (30 mL). The solid was chromatographed on silica gel, eluting with dichloromethane to yield the following, in order of elution. (i) 4-Methyl-7-aminocoumarin (7%; EtOH): mp 222 °C, ^1H NMR (acetone- d_6) 6.75 (d, $J = 8.6$ Hz, 1H, H-5), 6.65 (dd, $J = 8.6$ and 2.2 Hz, 1H, H-6), 6.50 (d, $J = 2.2$ Hz, 1H, H-8), 5.94 (q, $J = 1.1$ Hz, 1H, H-3), 2.38 (d, $J = 1.1$ Hz, 3 H, Me-4). Anal. Calcd for $\text{C}_{10}\text{H}_8\text{NO}_2$: C, 68.56; H, 5.18;

N, 8.00. Found: C, 68.33; H, 5.19; N, 7.93. (ii) 4-Methyl-5-hydroxyquinolin-2-one (8) (16%; MeOH): mp 300 °C; ¹HNMR (acetone-d₆) 7.28 (dd, J = 8.1 and 8.0 Hz, 1H, H-7), 6.80 (dd, J = 8.1 and 1.1 Hz, 1H, H-6 or H-8), 6.61 (dd, J = 8.0 and 1.1 Hz, 1H, H-6 or H-8), 6.28 (q, d = 1.2 Hz, 1H, H-3), 2.72 (d, J = 1.2 Hz, 3H, Me-4). Anal. Calcd for C₁₀H₈NO₂: C, 68.56; H, 5.18; N, 8.00. Found: C, 68.26; H, 5.15; N, 7.91.

Figures Captions

Fig. S1: ^1H NMR spectrum of the newly synthesized ligand (PAHMQ) in DMSO-d_6 .

Fig. S2: ^{13}C NMR spectrum of PAHMQ.

Fig. S3: ^1H NMR spectrum of PAHMQ in a DMSO-d_6 - D_2O mixture.

Fig. S4: Thermal curves of PAHMQ.

Fig. S5: Thermal curves of CoPAHMQ.

Fig. S6: Thermal curves of CuPAHMQ.

Fig. S7: Thermal curves of ZnPAHMQ.

Fig. S8: Morphological alterations of untreated MCF-7 cells (control)

Fig. S9: Morphological alterations of MCF-7 cells after 24 h treatment with serial concentrations PAHMQ.

Fig. S10: Morphological alterations of MCF-7 cells after 24 h treatment with serial concentrations of CoPAHMQ.

Fig. S11: Morphological alterations of MCF-7 cells after 24 h treatment with serial concentrations of CuPAHMQ.

Fig. S12: Morphological alterations of MCF-7 cells after 24 h treatment with serial concentrations of ZnPAHMQ.

Fig. S13: Morphological alterations of untreated MCF-10A cells (control)

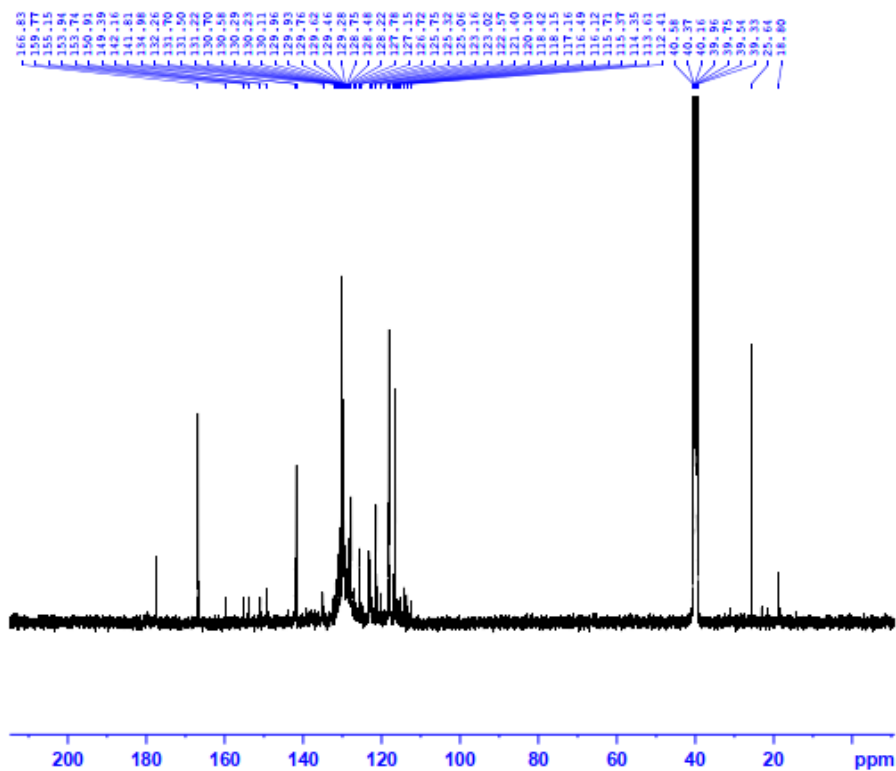
Fig. S14: Morphological alterations of MCF-10A cells after 24 h treatment with serial concentrations PAHMQ.

Fig. S15: Morphological alterations of MCF-10A cells after 24 h treatment with serial concentrations of CoPAHMQ.

Fig. S16: Morphological alterations of MCF-10A cells after 24 h treatment with serial concentrations of CuPAHMQ.

Fig. S17: Morphological alterations of MCF-10A cells after 24 h treatment with serial concentrations of ZnPAHMQ.

Rozan Zakaria-ligand Rt-carbon-DMSO-D



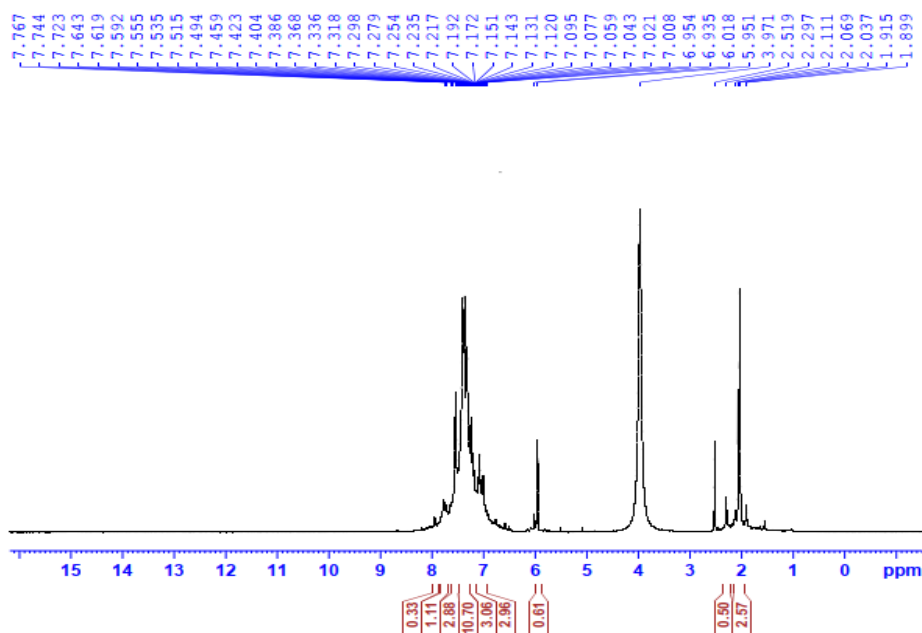
Current Data Parameters
 NAME Rozan Zakaria-ligand Rt-carbon-DMSO-D
 EXPNO 10
 PROCNO 1

F2 - Acquisition Parameters
 Date_ 20231118
 Time 22.12 h
 INSTRUM spect
 PROBRD 210MC18_0915 f
 PULPROG zgpg30
 TD 65536
 FIDRES 0.30000000
 SOLVENT DMSO
 NS 2000
 DS 4
 SWH 20298.641 Hz
 FIDRES 0.751898 Hz
 AQ 1.343188 sec
 RG 197.77
 CW 20.850 uVHz
 DE 6.50 uVHz
 TE 298.2 K
 D3 7.00000000 sec
 D31 0.20000000 sec
 TSD 1
 SFO1 100.6261331 MHz
 NS1 130
 F1 10.00 uVHz
 PLM1 07.00000000 W
 SFO2 400.2014626 MHz
 SFO3 100.6261331 MHz
 CPOW12 100.00000000 W
 PCPO2 90.00 uVHz
 PLM2 13.00000000 W
 PLM3 0.20000000 W
 PLM4 0.11710000 W

F2 - Processing parameters
 SI 32768
 SF 100.6261330 MHz
 WHW 0 EM
 SSB 0
 LB 1.00 Hz
 GB 0
 PC 1.00

Fig. S2

Rozan Zakaria-ligand Rt-D2O-RR



Current Data Parameters
 NAME Rozan Zakaria-ligand Rt-D2O-RR
 EXPNO 10
 PROCNO 1

F2 - Acquisition Parameters
 Date_ 20231118
 Time 11.10 h
 INSTRUM spect
 PROBRD 210MC18_0915 f
 PULPROG zgpg30
 TD 65536
 FIDRES 0.30000000
 SOLVENT DMSO
 NS 2000
 DS 4
 SWH 8012.810 Hz
 FIDRES 0.244851 Hz
 AQ 4.0824405 sec
 RG 10.97
 CW 42.400 uVHz
 DE 6.50 uVHz
 TE 298.0 K
 D3 1.00000000 sec
 TSD 1
 SFO1 400.2024712 MHz
 NS1 130
 F1 10.00 uVHz
 PLM1 13.00000000 W

F2 - Processing parameters
 SI 32768
 SF 400.2024712 MHz
 WHW 0 EM
 SSB 0
 LB 0.30 Hz
 GB 0
 PC 1.00

Fig. S3

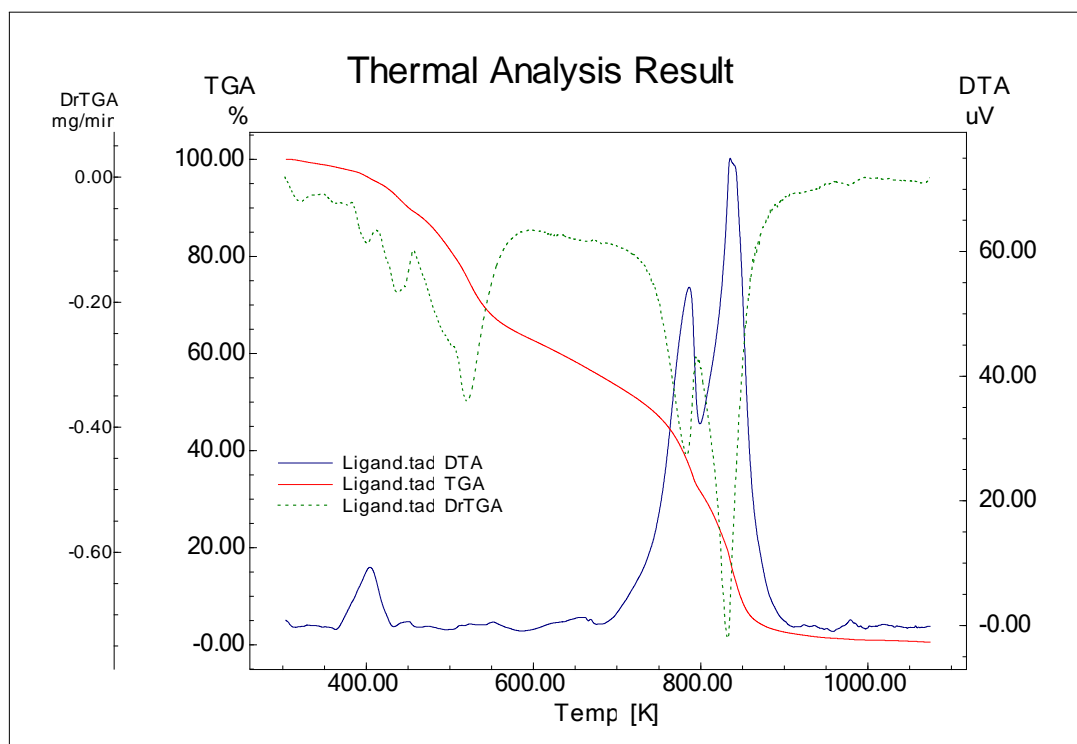


Fig. S4

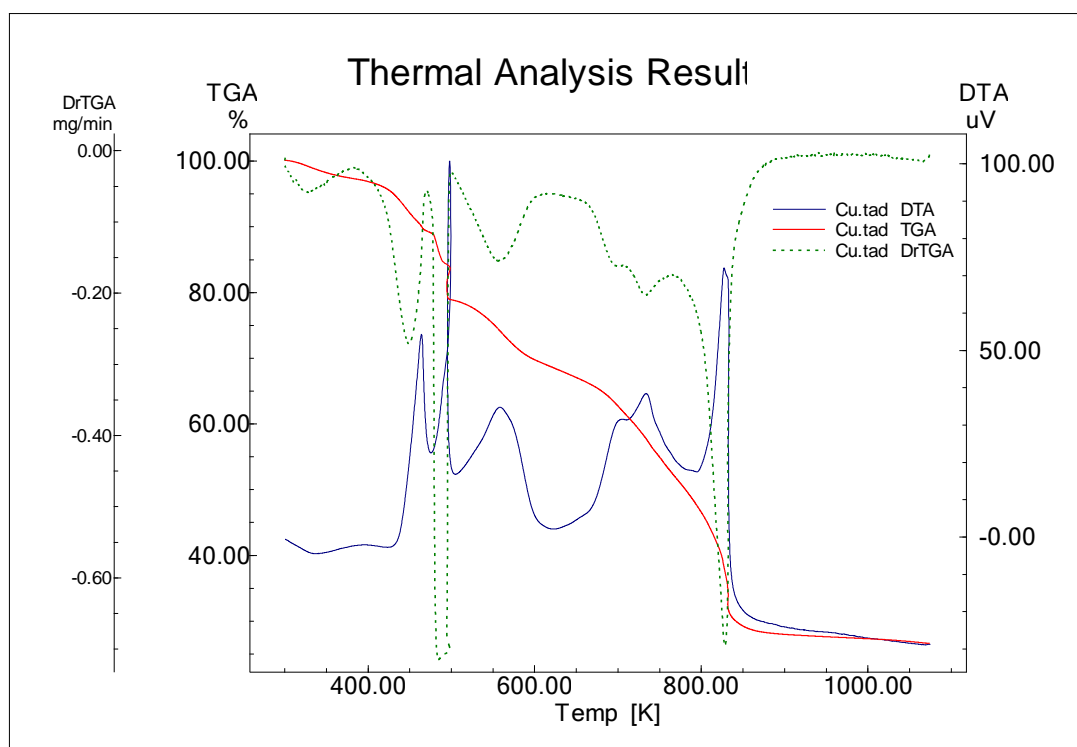


Fig. S5

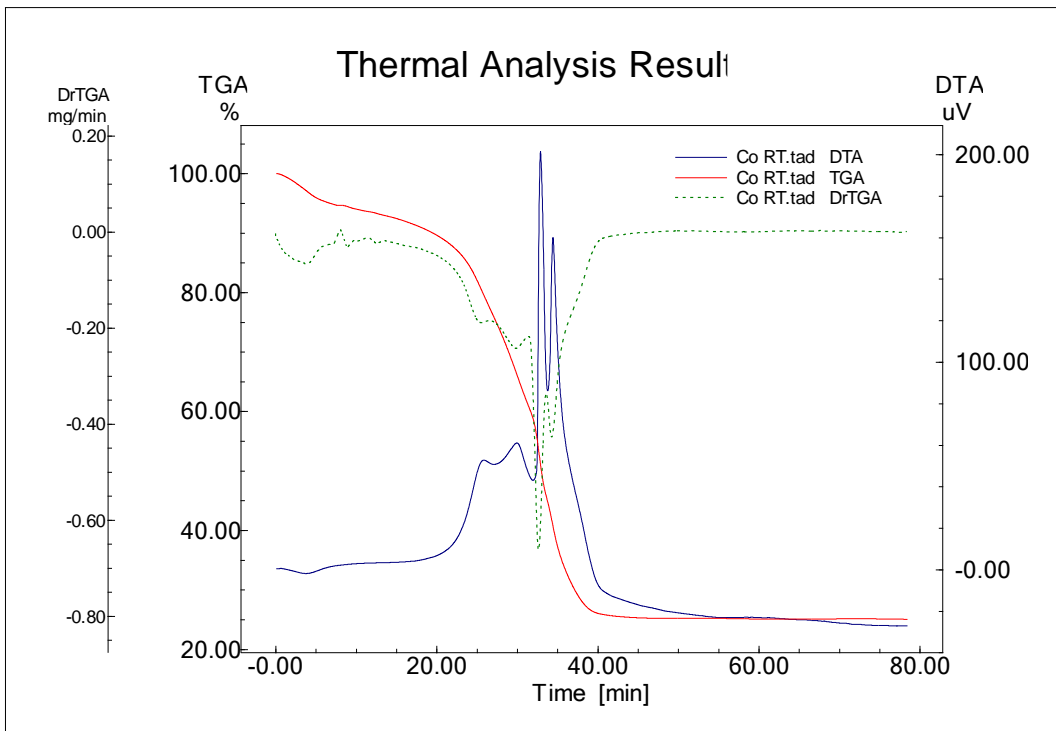


Fig. S6

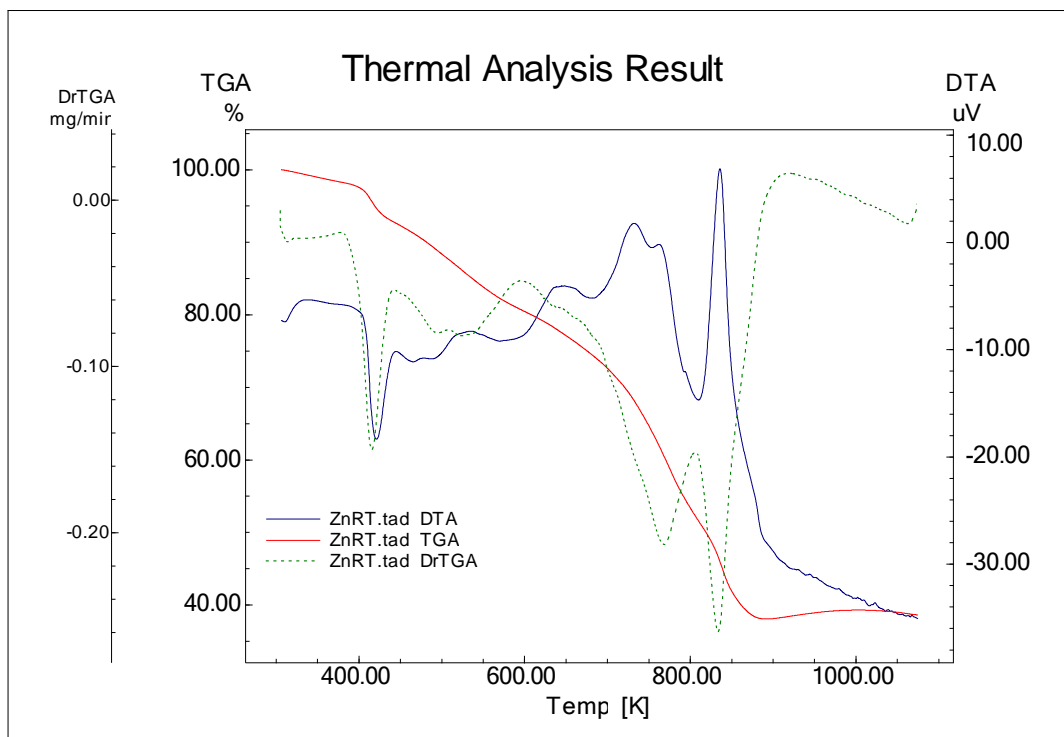
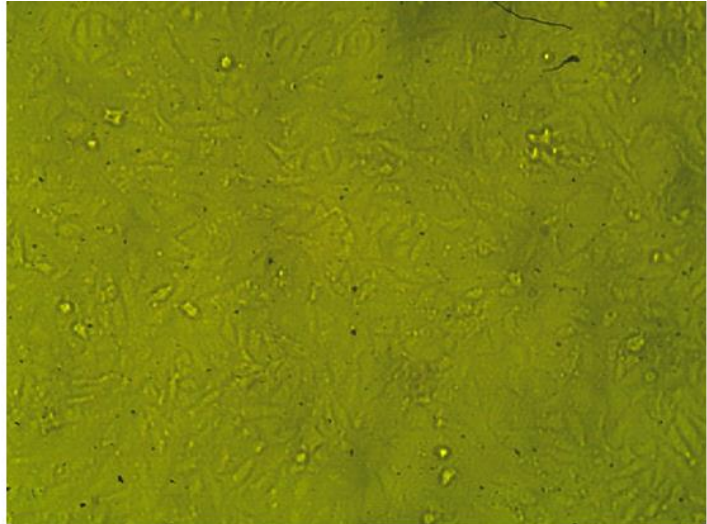


Fig. S7

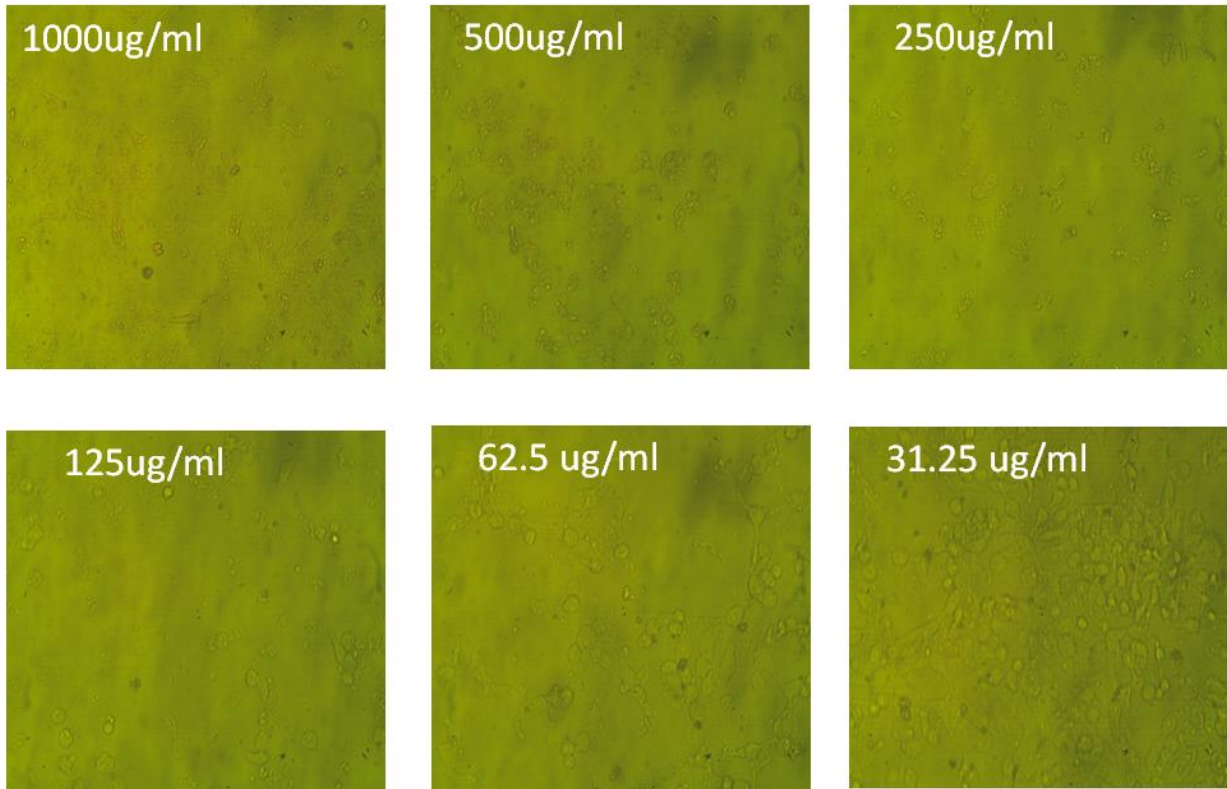


control
Mcf7 cells

Organism : *Homo sapiens*, human
Tissue : mammary gland, breast; derived from metastatic site: pleural effusion
Cell Type : epithelial
Culture Properties : adherent
Disease : adenocarcinoma
ATCC : HTB-22

Fig. S8

Effect of sample ligand on Mcf7 cells at different concentration



Effect of sample ligand on Mcf7 cells at different concentration

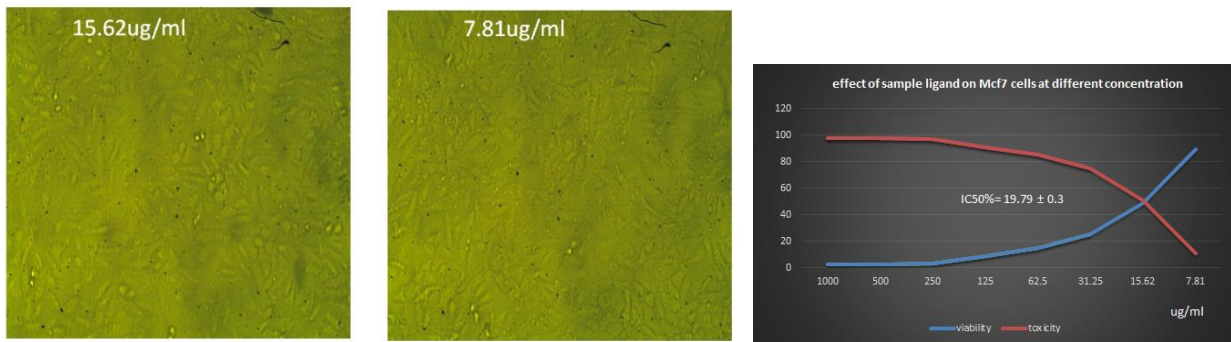
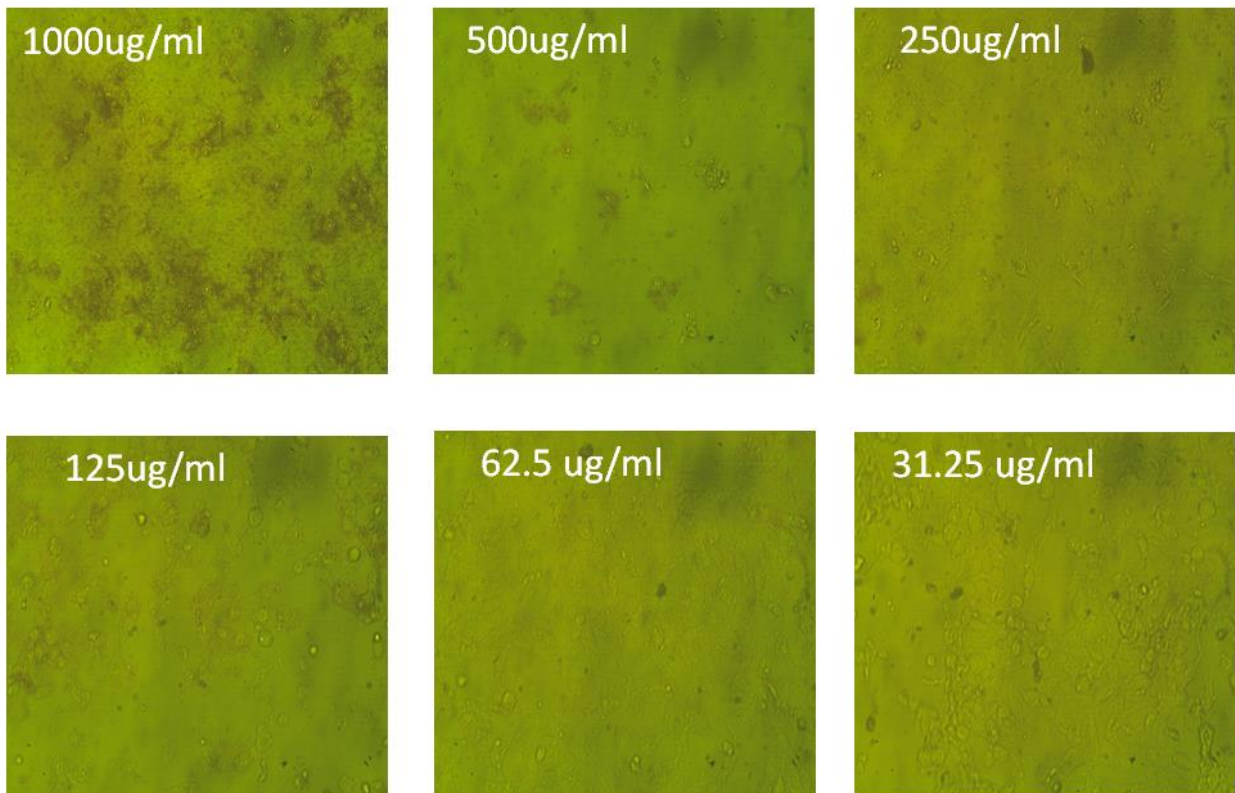


Fig. S9

Effect of sample Zn on MCF7 cells at different concentration



Effect of sample Zn on MCF7 cells at different concentration

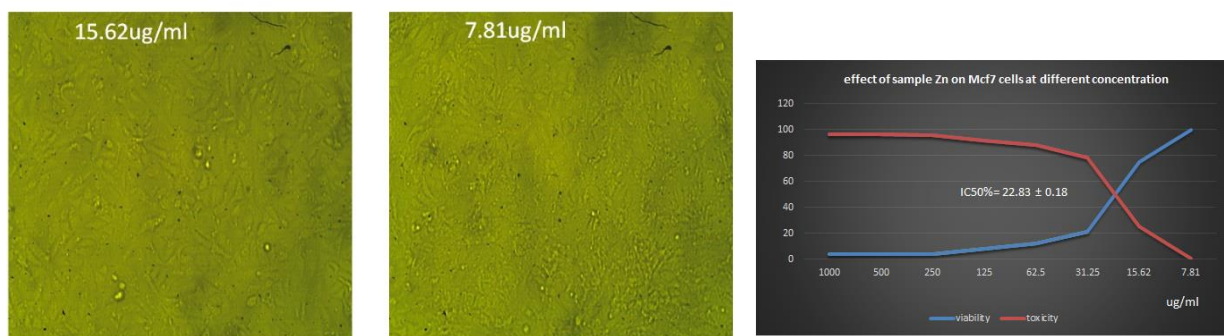
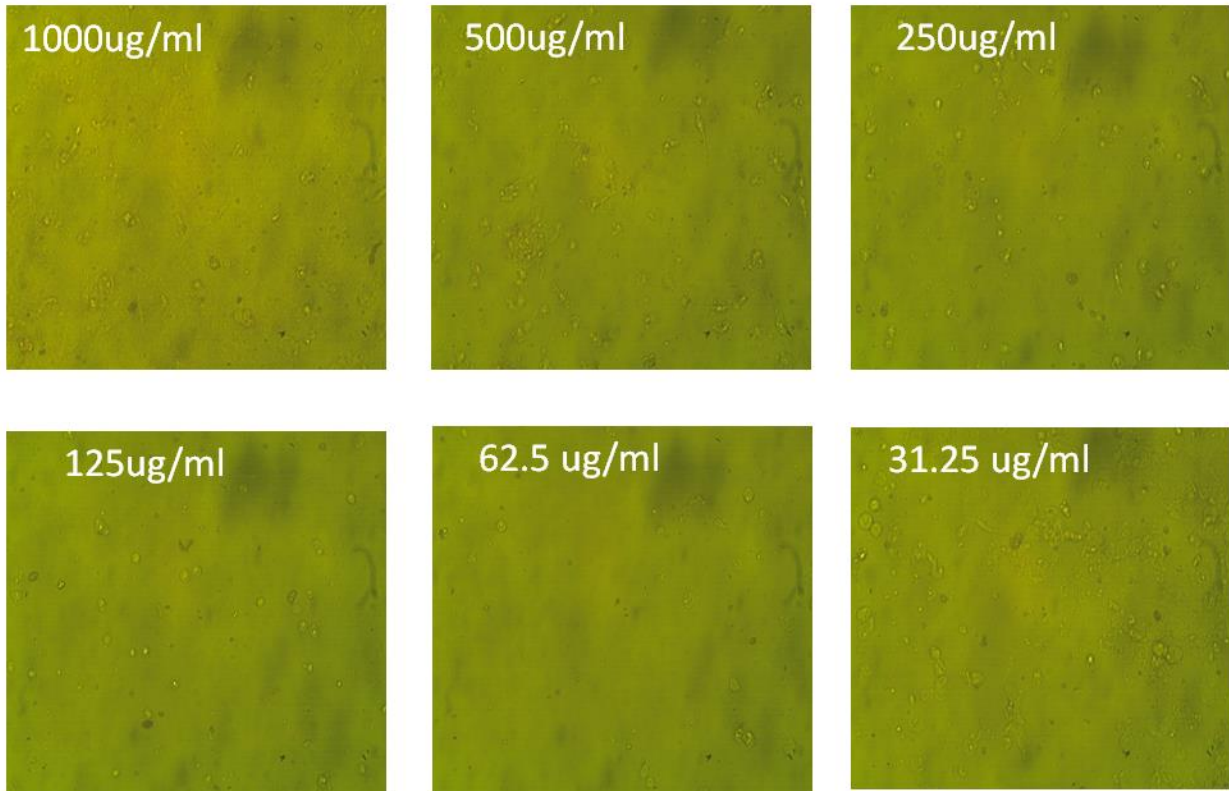


Fig. S10

Effect of sample cu on Mcf7 cells at different concentration



Effect of sample Cu on Mcf7 cells at different concentration

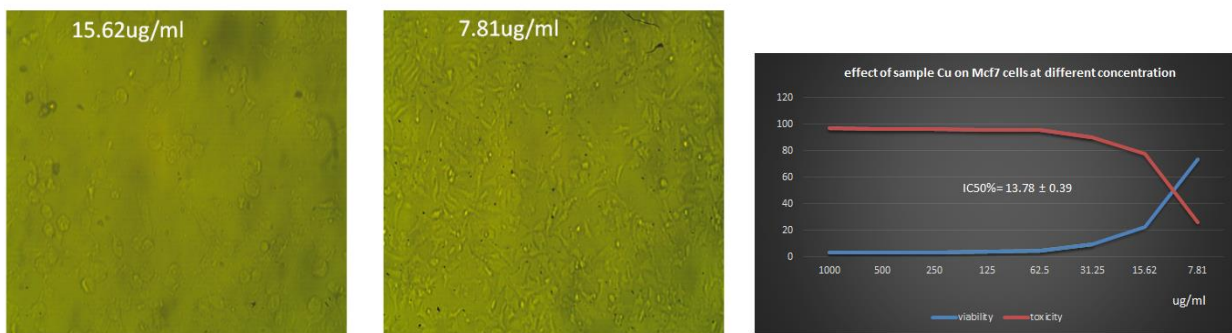
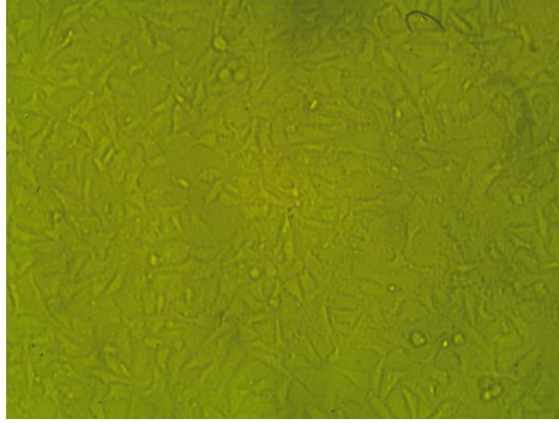


Fig. S11



**control
Mcf10A cells**

Organism : *Homo sapiens*, human
Tissue : Human mammary epithelial cell
Cell Type : epithelial
Culture Properties : adherent
ATCC : CRL-10317

Fig. S12

Effect of sample ligand RT on MCF10A cells at different concentration

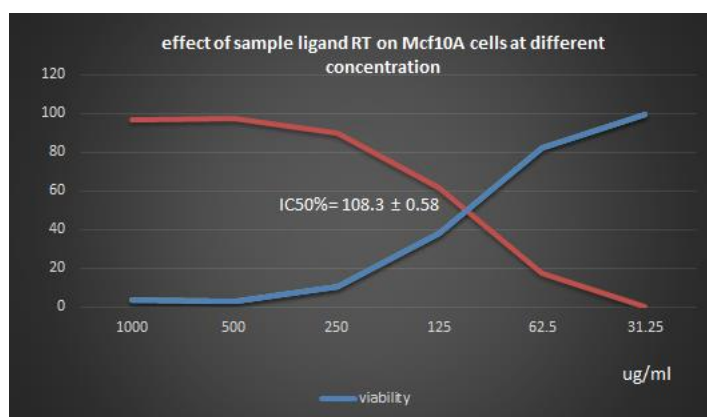
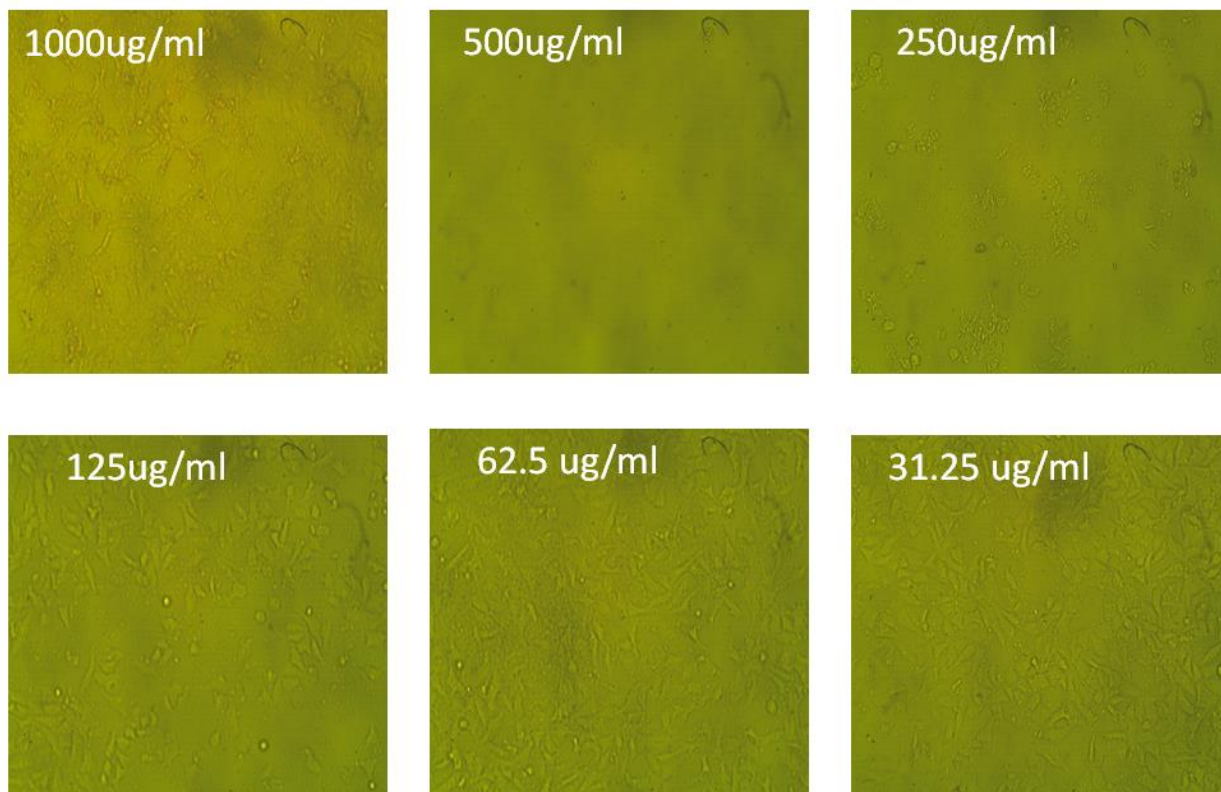


Fig. S13

Effect of sample Zn RT on MCF10A cells at different concentration

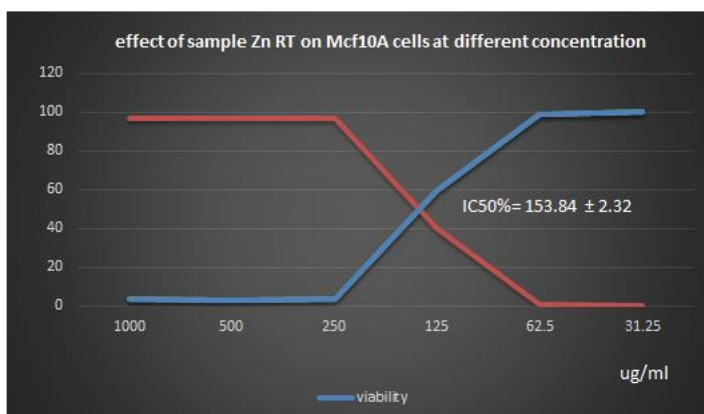
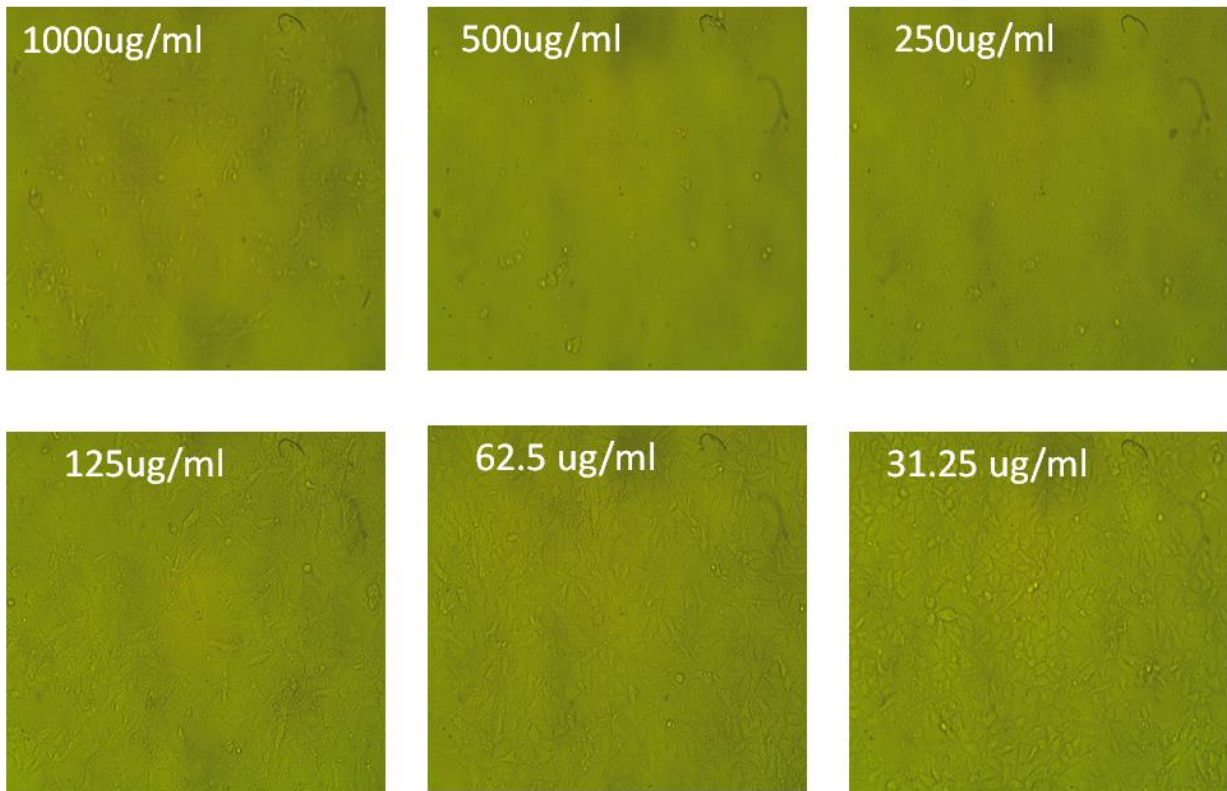
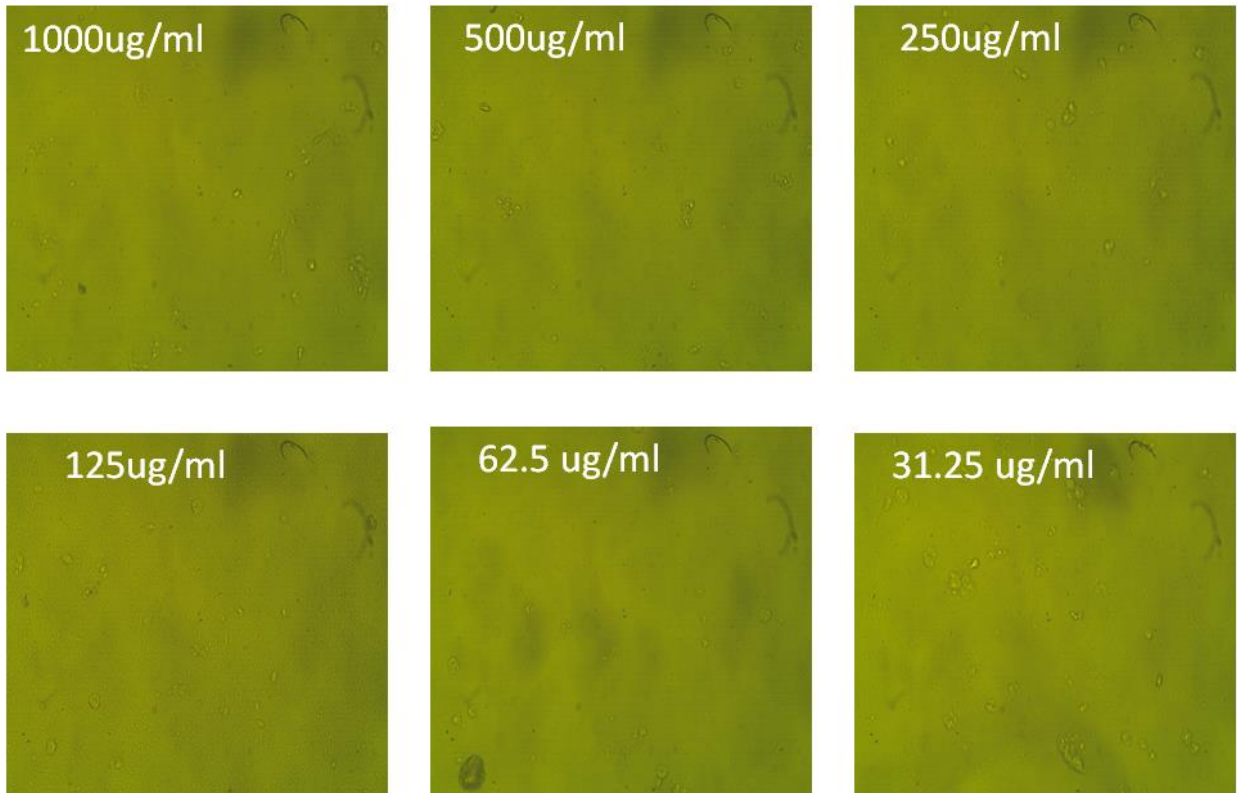


Fig. S14

Effect of sample Cu RT on MCF10A cells at different concentration



Effect of sample Cu RT on MCF10A cells at different concentration

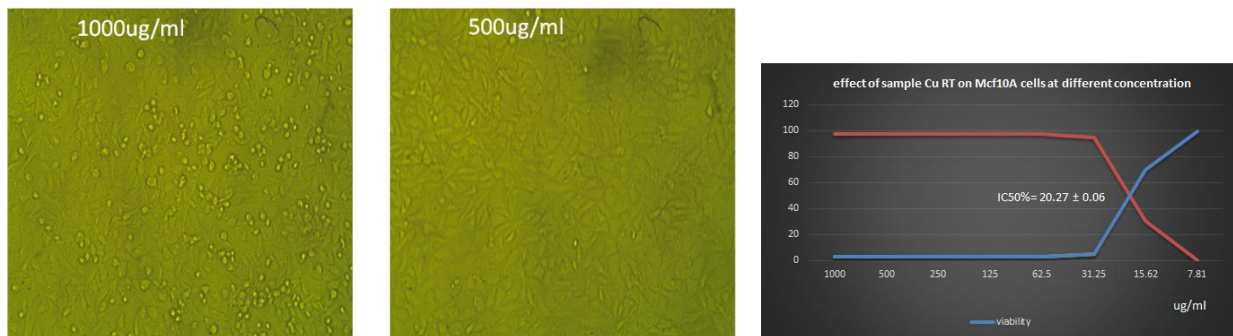


Fig. S15

Effect of sample Co RT on MCF10A cells at different concentration

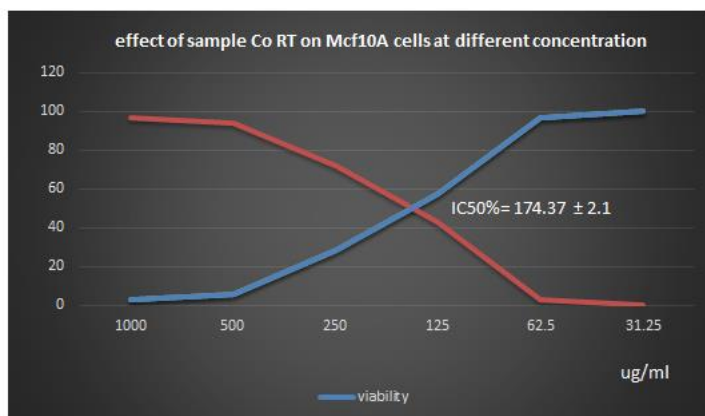
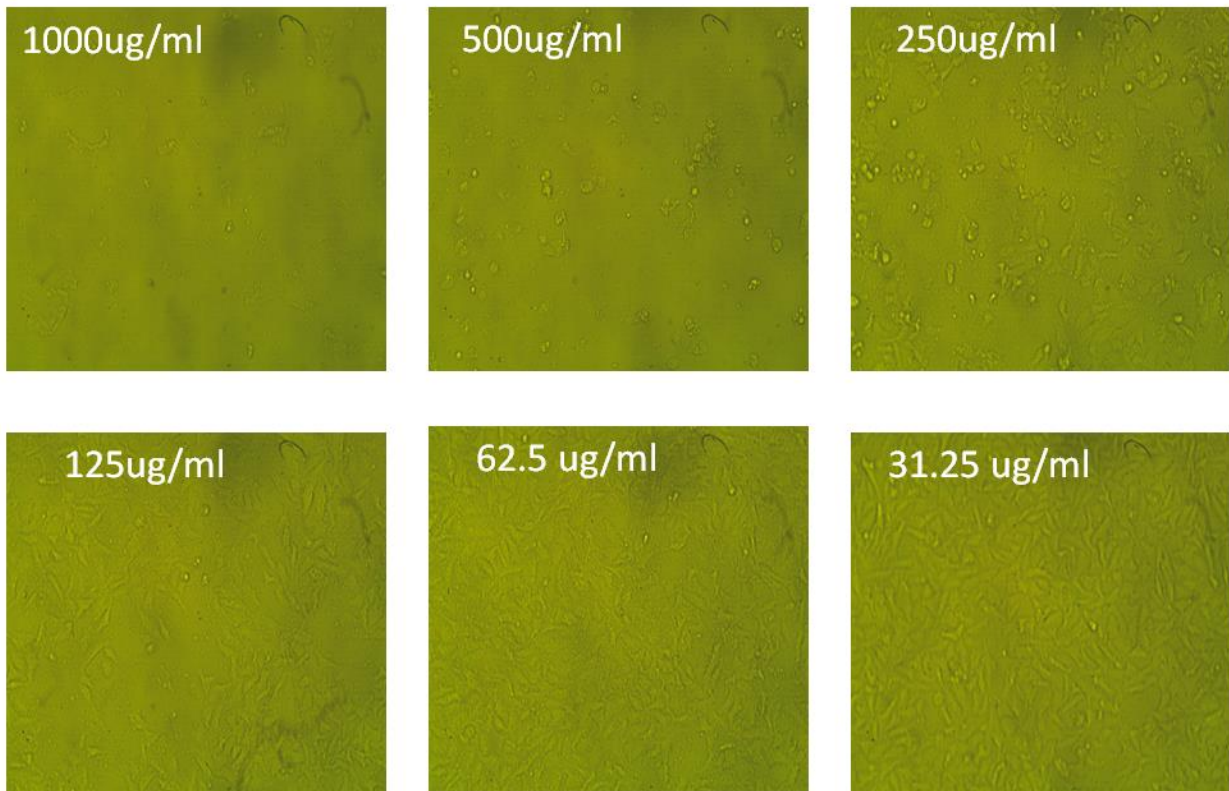
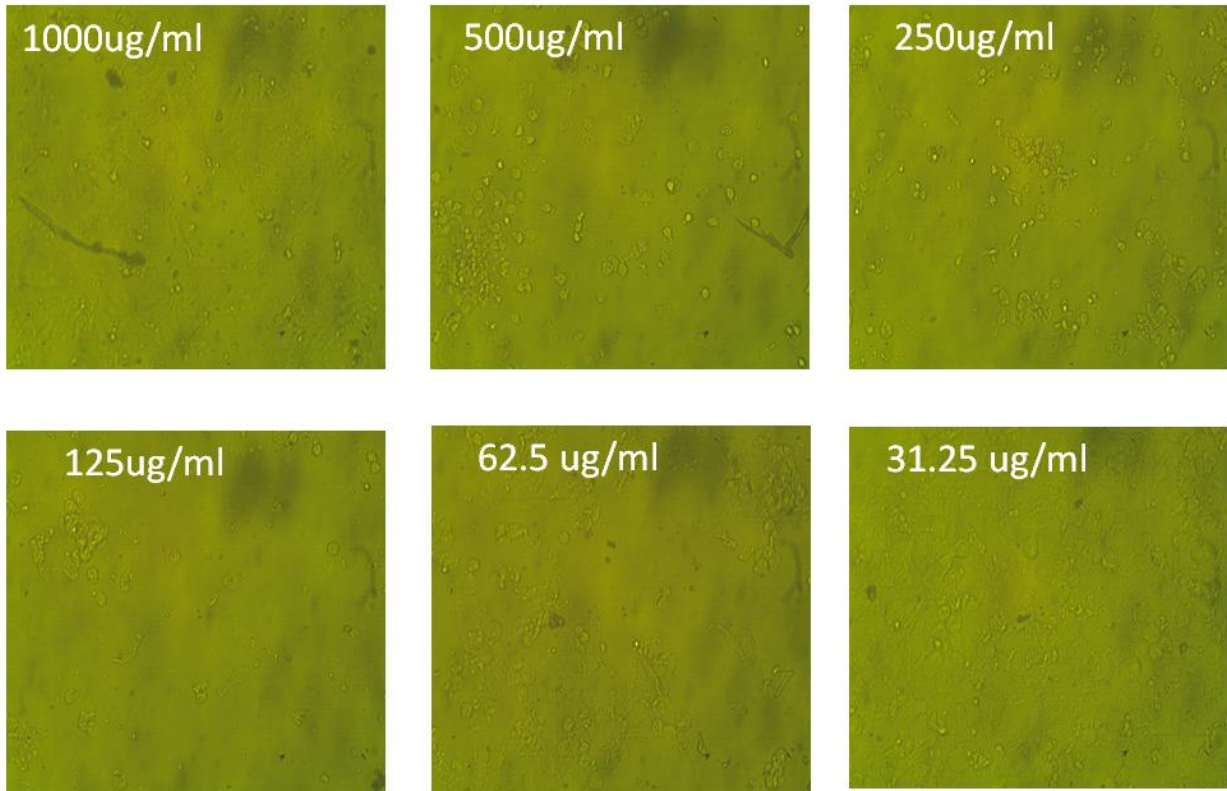


Fig. S16

Effect of sample co on Mcf7 cells at different concentration



Effect of sample Co on Mcf7 cells at different concentration

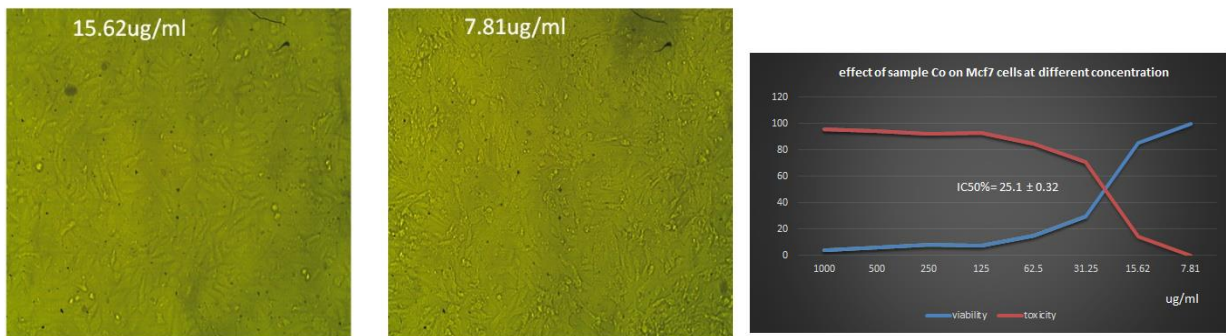


Fig. S17

Table S1: List of primers sequences used for RT-PCR analysis

Primers	Forward sequence	Reverse sequence
P53	5'-AACGGTACTCCGCCACC-3'	5'-CGTGTCACCGTCGTGGA-3'
Bax	5'-CTGAGCTGACCTTGGAGC-3'	5'-GACTCCAGCCACAAAGATG-3'
Bcl2	5'-TATAAGCTGTCGCAGAGGGGCTA-3'	5'-GTACTCAGTCATCCACAGGGCGAT-3'

Table S2: comparison between the anticancer activity of new Cu(II) complex with reported ones

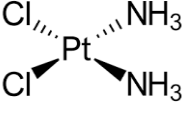
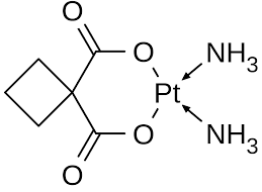
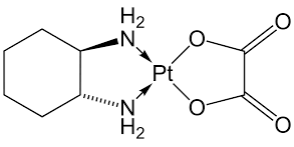
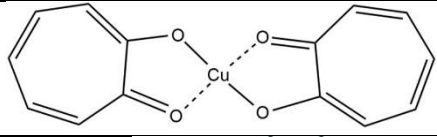
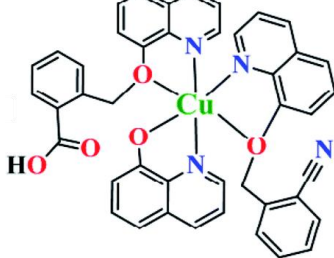
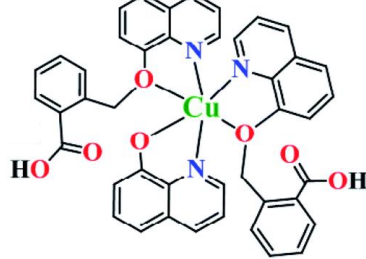
Nr	compound	Structure	IC ₅₀ (μM)	Ref.
1	Cisplatin		12.25 ± 0.35	[S1]
2	Carboplatin		73.48	[S2]
3	Oxaliplatin		21.92	[S2]
4	Cu(trp) ₂		18.32	[S3]
5	Cu(Hqmba)(qmbn)		10.91 ± 1.1	[S4]
6	Cu(Hqmba) ₂		13.89 ± 1.1	[S4]
7	CuPAHMQ		11.69	This work

Table S3 Results of molecular docking for two receptors.

Compounds	PDB ID	Receptors	Energy (kcal/mol)	Bonds formed between functional groups of component and protein residues	
				Functional groups	Residues
PAHMQ	3OCB	AKT1 kinase	-6.4712	O, cyclohexone	Thr 305, Lys 389
CuPAHMQ			-8.4891	H ₂ O, Benzene, Cl,	Glu 322, Lys 386, Glu 365, Met 363
Selumetinib			-7.8964	Br, Benzene, OH	Thr 195, Phe 161, Asp 274
PAHMQ	3QX3	Topoisomerase II inhibitors	-6.0931	Benzene, N, O, Cyclohexone	Asn 867, Gln 742, Lys 739, Gly 871, Asn 786
CuPAHMQ			-51.3505	N, H ₂ O, Benzene, Cl	His 777, Asp 559, Glu 477, Gly 504, Lys 505
Doxorubicin			-5.9348	NH ₃ , O, OH	Gly 737, Gln 742, Lys 739, Arg 945, Asn 786

[S1]

[S2] Alami, N., Li, Z., Engel, J., & Leyland-Jones, B. (2007). Comparative preclinical antiproliferative activity of lobaplatin vs cisplatin, carboplatin, oxaliplatin and satraplatin in breast and ovarian cancers. *Cancer Research*, 67(9_Supplement), 4780-4780.

[S3] Balsa, L. M., Ruiz, M. C., de la Parra, L. S. M., Baran, E. J., & León, I. E. (2020). Anticancer and antimetastatic activity of copper (II)-tropolone complex against human breast cancer cells, breast multicellular spheroids and mammospheres. *Journal of Inorganic Biochemistry*, 204, 110975.

[S4] Ali, A., Banerjee, S., Kamaal, S., Usman, M., Das, N., Afzal, M., ... & Ahmad, M. (2021). Ligand substituent effect on the cytotoxicity activity of two new copper (ii) complexes bearing 8-hydroxyquinoline derivatives: Validated by MTT assay and apoptosis in MCF-7 cancer cell line (human breast cancer). *RSC advances*, 11(24), 14362-14373.